

Supporting Information

Construction of a quencher-free cascade amplification system for highly specific and sensitive detection of serum circulating miRNAs

Li-juan Wang^{a,†}, Ming Ren^{a,†}, Hou-xiu Wang^{a,†}, Jian-Ge Qiu^b, BingHua Jiang^{b,*} and Chun-yang Zhang^{a,*}

^a College of Chemistry, Chemical Engineering and Materials Science, Collaborative Innovation Center of Functionalized Probes for Chemical Imaging in Universities of Shandong, Key Laboratory of Molecular and Nano Probes, Ministry of Education, Shandong Provincial Key Laboratory of Clean Production of Fine Chemicals, Shandong Normal University, Jinan 250014, China.

^b Academy of Medical Sciences, Zhengzhou University, Zhengzhou, Henan, 450000, China.

[†] These authors contributed equally.

*To whom correspondence should be addressed. E-mail: cyzhang@sdsu.edu.cn;

bhjiang@zzu.edu.cn; Tel.: +86 0531-86186033; Fax: +86 0531-82615258.

Table of Contents

Optimization of reaction buffer.....	S3
Optimization of the concentration of hairpin probe.....	S4
Optimization of the amount of lambda exonuclease.....	S5
Optimization of reaction time.....	S6
The qRT-PCR measurement.....	S6
Analysis of circulating miR-486-5p in human serum samples.....	S8
References.....	S8

1. Optimization of reaction buffer.

Different enzymes always require different reaction conditions to achieve their optimal enzyme activities. In the proposed strategy, three kinds of tool enzymes (i.e., DNA polymerase I, Nb.BtsI, and lambda exonuclease) are involved in the quencher-free cascade amplification system, and thus the reaction buffer should be optimized to achieve the best assay performance. In this research, three kinds of reaction buffers are involved, which are corresponding to the above three enzymes, including buffer 1 (i.e., NEBuffer 2, the reaction buffer of DNA polymerase I), buffer 2 (i.e., CutSmart buffer, the reaction buffer of Nb.BtsI), and buffer 3 (i.e., lambda exonuclease reaction buffer). As shown in Figure S1, no distinct fluorescence signals are detected in the presence of either buffers 1 + 2 + 3 or buffer 3, indicating no occurrence of amplification reaction. In contrast, a high fluorescence signal is detected in the presence of buffers 1 + 3, indicating that the quencher-free cascade amplification is initiated to release abundant 2-AP molecules for the generation of an enhanced fluorescence signal. Therefore, the mixture of buffers 1 and 3 is used in the subsequent research.

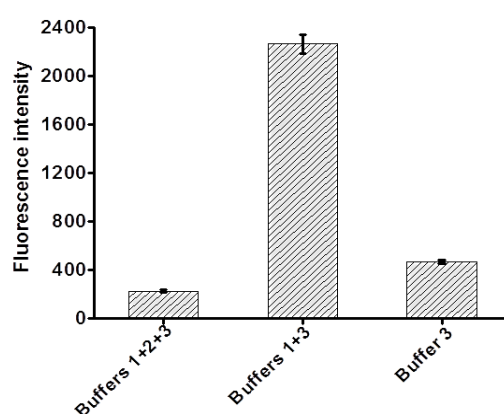


Figure S1. Variance of fluorescence intensity in response to different reaction buffers. Buffer 1 is NEBuffer 2, buffer 2 is CutSmart buffer, and buffer 3 is lambda exonuclease reaction buffer. The concentration of miR-486-5p is 10 nM. Error bars show the standard deviations of three

independent experiments.

2. Optimization of the concentration of hairpin probe.

In this assay, the nucleotide of 2-aminopurine (2-AP) is strategically employed as the quencher-free fluorophore, and the hairpin probe is designed to contain two 2-AP substitutions. Therefore, the concentration of hairpin probe will directly determine the total number of fluorescent molecules (i.e., 2-AP molecules) in the cascade amplification system and will significantly affect the detection sensitivity. As shown in Figure S2, when the hairpin probe concentration increases from 50 to 300 nM, the fluorescence intensity enhances correspondingly, and reaches a plateau beyond the concentration of 300 nM. Thus, 300 nM is selected as the optimal concentration of hairpin probe.

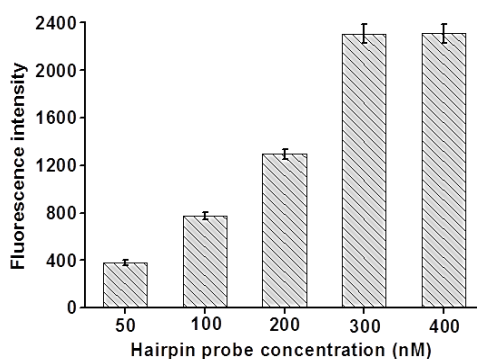


Figure S2. Variance of fluorescence intensity in response to different concentrations of hairpin probe. The concentration of miR-486-5p is 10 nM. Error bars show the standard deviations of three independent experiments.

3. Optimization of the amount of lambda exonuclease.

In this assay, lambda exonuclease can catalyze the cleavage of hairpin probes upon their hybridization with binding probes, initiating the recycling cleavage amplification (cycle II) to release abundant 2-AP molecules. Thus, the amount of lambda exonuclease may influence the efficiency of whole quencher-free cascade amplification reaction. As shown in Figure S3, the fluorescence intensity enhances with the increasing amount of lambda exonuclease from 0.1 to 1 U, and reaches the maximum value at the amount of 1 U, followed by the decrease at the amount of 2 U, because lambda exonuclease may degrade the nonphosphorylated substrates at a greatly reduced rate¹ and the excessive amount of lambda exonuclease may induce the nonspecific cleavage to decrease the amplification efficiency. Therefore, 1 U of lambda exonuclease is used in the subsequent experiments.

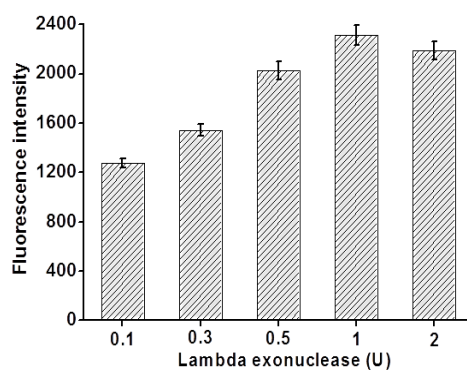


Figure S3. Variance of fluorescence intensity in response to different amounts of lambda exonuclease. The concentration of miR-486-5p is 10 nM. Error bars show the standard deviations of three independent experiments.

4. Optimization of reaction time.

Considering the high efficiency of the quencher-free cascade amplification system, the reaction time should be optimized to reduce the assay time. As shown in Figure S4, the fluorescence intensity increases monotonically with reaction time, and reaches a plateau at 45 min. Thus, the reaction time of 45 min is used in the subsequent experiments.

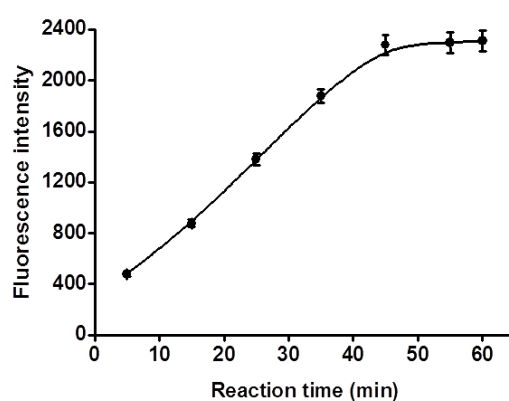


Figure S4. Variance of fluorescence intensity with reaction time. The concentration of miR-486-5p is 10 nM. Error bars show the standard deviation of three independent experiments.

5. The qRT-PCR measurement.

We used the standard qRT-PCR to verify the accuracy and reliability of the proposed method. After the reverse transcription of target miRNA, the reaction products were subjected to quantitative PCR analysis. As shown in Figure S5, the real-time fluorescence measurements in response to different concentrations of miR-486-5p were performed by using SYBR Green I as the fluorescent indicator. When the miR-486-5p concentration increases from 0 to 1 nM, the real-time fluorescence intensity enhances in a sigmoidal fashion. The threshold cycle (C_T) value (i.e., the fractional cycle number at which amount of amplified target reaches a fixed threshold)² exhibits a linear correlation with the logarithm of miR-486-5p concentration in the range from 100 aM to 1

nM, and the regression equation is $C_T = -12.70 - 2.74 \log_{10} C_{\text{miR-486-5p}}$ with a correlation coefficient (R^2) of 0.9966, where C is the concentration of miR-486-5p (M).

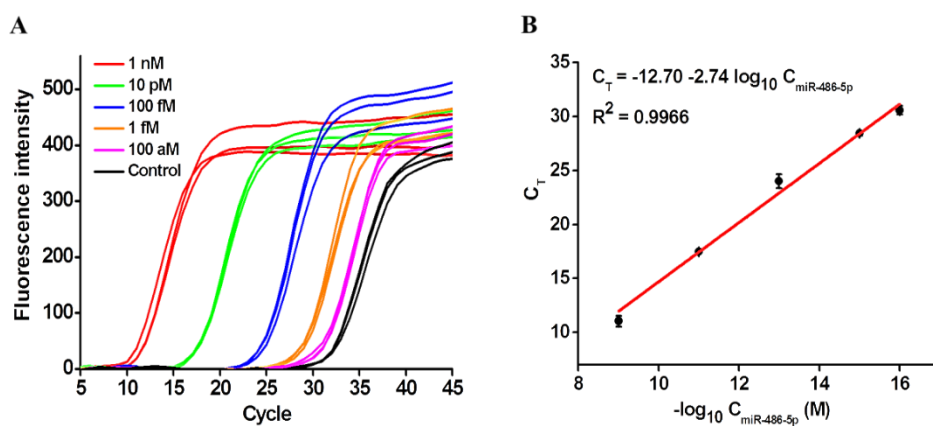


Figure S5. (A) Real-time fluorescence monitoring of the PCR amplification reaction in response to different concentrations of miR-486-5p in the range from 0 to 1 nM. (B) Linear relationship between the C_T value and the logarithm of miR-486-5p concentration. Error bars show the standard deviation of three independent experiments.

6. Analysis of circulating miR-486-5p in human serum samples.

Table S1. Detection of serum circulating miR-486-5p from five healthy persons and five NSCLC patients.

sample	fluorescence intensity	miR-486-5p concentration (pM, by this method)	median concentration (pM)	C_T value	miR-486-5p concentration (pM, by RT-PCR)	median concentration (pM)
normal 1	1687.17 ± 65.60	16.29 ± 1.40	12.78	16.72 ± 0.11	18.35 ± 1.41	14.32
normal 2	1675.62 ± 62.62	14.33 ± 1.22		16.84 ± 0.06	16.53 ± 1.37	
normal 3	1648.11 ± 59.5	10.56 ± 1.08		17.26 ± 0.10	11.66 ± 1.1	
normal 4	1665.31 ± 61.31	12.78 ± 1.10		16.97 ± 0.12	14.85 ± 1.26	
normal 5	1642.57 ± 60.52	9.93 ± 1.02		17.41 ± 0.09	10.23 ± 1.11	
patient 1	1225.12 ± 48.02	0.10 ± 0.02	0.34	22.92 ± 0.13	0.10 ± 0.12	0.39
patient 2	1320.66 ± 53.48	0.28 ± 0.48		21.57 ± 0.08	0.31 ± 0.58	
patient 3	1410.15 ± 58.61	0.75 ± 0.61		20.24 ± 0.10	0.95 ± 0.68	
patient 4	1370.07 ± 56.05	0.48 ± 0.05		20.98 ± 0.14	0.51 ± 0.07	
patient 5	1200.02 ± 45.14	0.07 ± 0.14		22.92 ± 0.15	0.10 ± 0.23	

References

- (1) Little, J. W. Lambda Exonuclease. *Gene Amplif. Anal.* **1981**, 2, 135-145.
- (2) Livak, K. J.; Schmittgen, T. D. Analysis of Relative Gene Expression Data Using Real-Time Quantitative PCR and the $2^{-(\Delta\Delta C(T))}$ Method. *Methods* **2001**, 25, 402-408.